


## Effects of micro-bubble aeration on the pollutant removal and energy-efficient process in a floc–granule sludge coexistence system

Minghui Liu<sup>a</sup>, Ju Wang<sup>a</sup> and Zhaoxu Peng <sup>a,b,\*</sup>

<sup>a</sup> School of Water Conservancy and Transportation, Zhengzhou University, Kexue Road 100, Zhengzhou 450001, China

<sup>b</sup> Faculty of Civil Engineering and Geosciences, Section Sanitary Engineering, Department of Water Management, Delft University of Technology, Stevinweg 1, Delft, South Holland 2628 CN, The Netherlands

\*Corresponding author. E-mail: pzx@zzu.edu.cn

 ZP, 0000-0002-7189-0819

### ABSTRACT

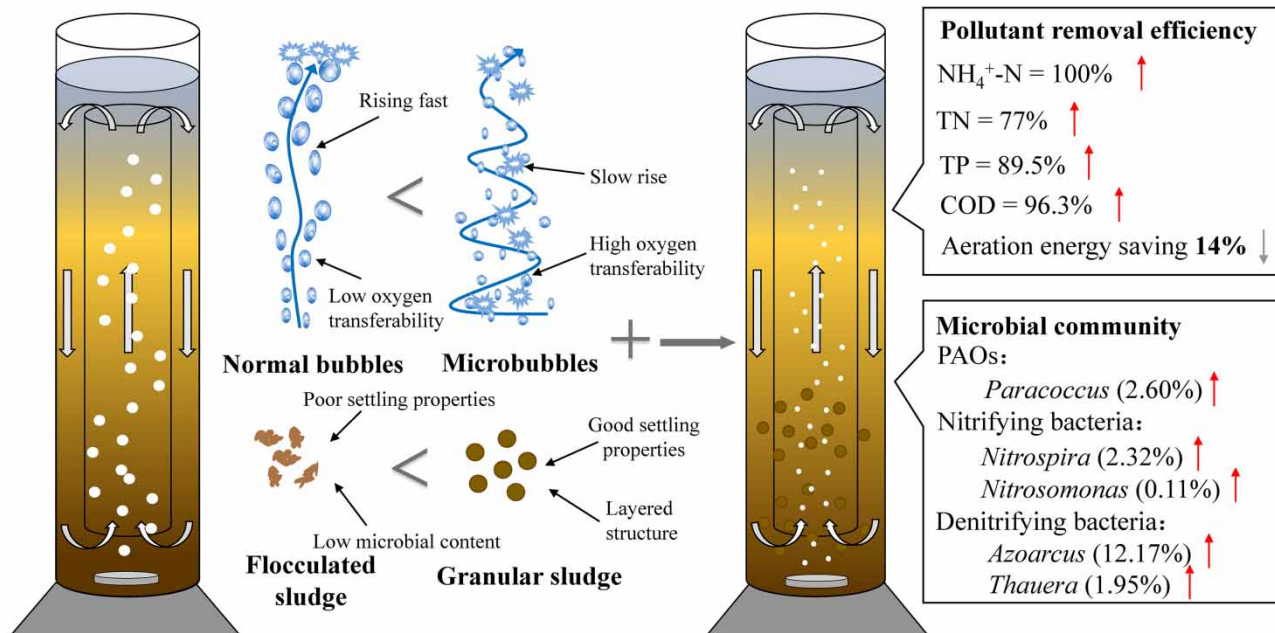
To investigate energy-saving approaches in wastewater treatment plants and decrease aeration energy consumption, this study successfully established a floc–granule coexistence system in a sequencing batch airlift reactor (SBAR) employing micro-bubble aeration. The analysis focused on granule formation and pollutant removal under various aeration intensities, and compared its performance with a traditional floc-based coarse-bubble aeration system. The results showed that granulation efficiency was positively associated with aeration intensity, which enhanced the secretion of extracellular polymeric substances (EPSs) and facilitated granule formation. The SBAR with the micro-aeration intensity of 30 mL·min<sup>-1</sup> showed the best granulation performance (granulation efficiency 52.6%). In contrast to the floc-based system, the floc–granule coexistence system showed better treatment performance, and the best removal efficiencies of NH<sub>4</sub><sup>+</sup>-N, TN, and TP were 100.0, 77.0, and 89.5%, respectively. The floc–granule coexistence system also enriched higher abundance of nutrients removal microbial species, such as *Nitrosomonas* (0.05–0.14%), *Nitrospira* (0.14–2.32%), *Azoarcus* (2.95–12.17%), *Thauera* (0.43–1.95%), and *Paracoccus* (0.76–2.89%). The energy-saving potential was evaluated, which indicated it is feasible for the micro-aeration floc–granule coexistence system to decrease the aeration consumption by 14.4% as well as improve the effluent.

**Key words:** energy saving, granular sludge, micro-bubble, sequencing batch airlift reactor

### HIGHLIGHTS

- A floc–granule sludge coexistence system was constructed in an SBAR system by micro-bubble aeration.
- Excessive aeration favors granular sludge formation, but not phosphorus removal.
- Floc–granule sludge coexistence systems have better functional bacterial genera and energy-saving potential compared to flocculated sludge systems.

## GRAPHICAL ABSTRACT



## 1. INTRODUCTION

Electricity, fuel, and chemical agents are the main possible energy sources used in urban wastewater treatment facilities. Electricity is mainly utilized for processes such as lifting sewage and sludge, supplying oxygen, and stabilizing and dewatering sludge. The electrical consumption of aeration system accounts for 30–50% of the total energy consumption in the entire plant, primarily attributed to the nitrification of  $\text{NH}_4^+\text{-N}$  and oxidation of organic matter, which is one of the major electricity-consuming components in urban wastewater treatment plants (WWTPs). To challenge the global climate change, how to improve wastewater treatment performance while reducing energy consumption has become a pressing issue.

In recent years, researchers have developed novel nitrogen removal processes such as partial nitrification (PN) and anaerobic ammonium oxidation (Anammox) to effectively reduce the energy consumption associated with nitrification (Kartal *et al.* 2010). However, the extended generation time of anaerobic ammonium oxidation bacteria (AnAOB) and the low concentration of  $\text{NO}_2^-\text{-N}$  in WWTPs are crucial factors that limit the application of Anammox in mainstream treatment processes (Wang *et al.* 2018). Aerobic granular sludge (AGS), as another emerging energy-efficient technology, offers advantages such as excellent settleability, high microbial abundance, diverse microbial communities, and strong shock loading tolerance compared to conventional floc-based activated sludge (Liu *et al.* 2009). The unique layered structure of granular sludge facilitates the efficient uptake of organic matter for phosphorus release during the anaerobic phase, and enables simultaneous nitrification–denitrification during the aerobic phase. This not only reduces energy consumption associated with organic matter oxidation but also optimizes nitrogen removal efficiency (Li *et al.* 2008; Bassin *et al.* 2012). To date, more than 100 WWTPs based on AGS technology, have been used in practical application worldwide, making significant contributions to energy conservation and reduction.

Currently, wastewater biological treatment technologies mostly rely on a continuous flow activated sludge process, which faces significant challenges in achieving complete sludge granulation. However, it is relatively easier to achieve partial sludge granulation, thus forming a coexistence state of flocculent and granular sludge. The sequencing batch reactor (SBR) is considered an ideal reactor to promote sludge granulation. Through the intermittent inflow mode and decreasing sedimentation time, SBR can create feast/famine environment and hydraulic selection pressure, providing favorable conditions for granulation (Show *et al.* 2012; Zhou *et al.* 2014). The SBAR is an improved SBR process, which incorporates an airlift device to enhance both fluid shear forces and mass transfer between the gas and liquid phases. Aeration cannot only provide dissolved oxygen (DO) for the oxidation of  $\text{NH}_4^+\text{-N}$  but also promote mixing. Furthermore, the hydraulic shear force indirectly contributes to form the granular sludge (Chen *et al.* 2017). However, high aeration intensity results in higher energy consumption,

while low aeration intensity may lead to inadequate pollutant removal. Therefore, it is essential to explore the optimal aeration intensity that can simultaneously promote granular sludge formation, achieve efficient pollutant removal, and minimize energy consumption.

Moreover, to enhance the oxygen transfer efficiency and reduce aeration energy consumption, micro-bubble aeration systems are commonly employed in WWTPs (Khuntia *et al.* 2012). Compared to the coarse-bubble aeration systems, the micro-bubble showed slower rising velocity and longer retention time, resulting in a larger gas–liquid mass transfer area and higher oxygen transfer efficiency (Cheng *et al.* 2016). There is a promising potential for AGS systems based on micro-bubble aeration to meet the dual requirements of effluent quality and energy consumption. However, there is limited research available in this field currently.

This study aims to investigate an energy-efficient nutrients removal process that combines micro-bubble aeration with AGS. A laboratory-scale SBAR reactor was utilized to explore the effects of different aeration intensities on the granulation process and the pollutant removal performance. By comparing its performance with that of a conventional coarse-bubble floc-based sludge, the potential of the combined system to improve effluent quality and reducing energy consumption was evaluated.

## 2. MATERIALS AND METHODS

### 2.1. Experimental setup and operation

The experimental setup is shown in Figure 1. The SBAR was made of organic glass with the height of 42 cm, inner diameter of 6.8 cm and effective volume of 1.2 L. The aeration discs were located at the bottom, and the aeration intensity was regulated using a rotor flowmeter. S1, S2, and S3 were aerated by micro-bubble aeration discs with the aeration intensities of 10, 20, and 30 mL·min<sup>-1</sup>, respectively. R2 was aerated by a conventional coarse-bubble aeration disc with the aeration intensity of 20 mL·min<sup>-1</sup>. A custom-made columnar internal circulation pipe with an inner diameter of 4.6 mm and a thickness of 2 mm was installed. The volume exchange ratio of each cycle was 0.5.

The inflow, aeration, settling time, and other parameters were automatically controlled by dual-time relays. Each cycle lasts for 8 h, the detailed operating conditions within each cycle are shown in Table 1. The idle stage is mainly to flexibly adjust the length of the operating cycle, but also to facilitate the recovery of sludge activity. At the 25th day, the sedimentation time for S1, S2, and S3 systems was reduced from 10 to 5 min, while the idle time was extended by 5 min with all other conditions remaining the same. The reactors were operated at room temperature (25 ± 2 °C). During the experiment, the inside surface of reactor were periodically cleaned to prevent biofilm proliferation.

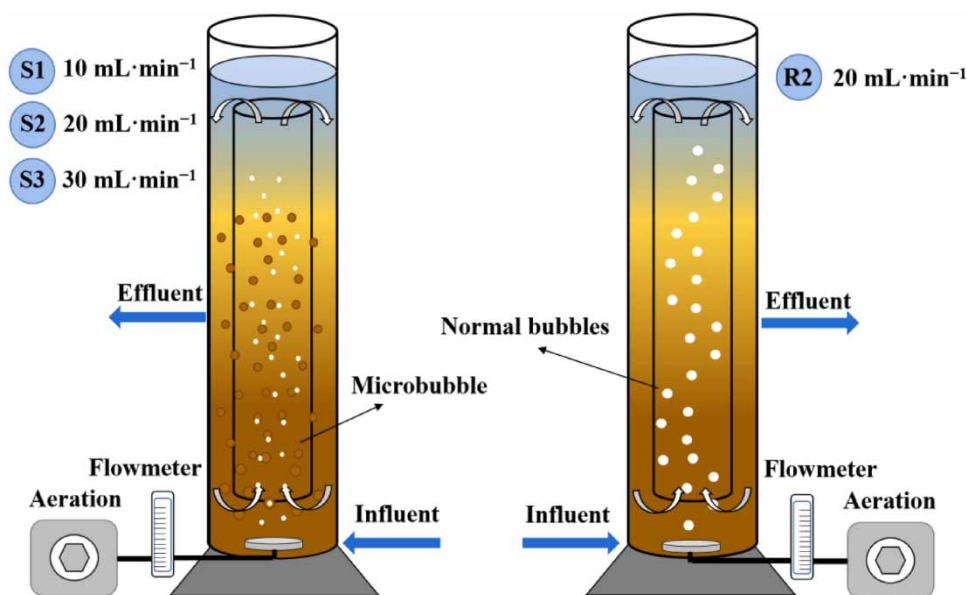


**Figure 1** | S1, S2, and S3 (micro-bubble) floc–granule sludge reactors, and R2 (normal bubble) flocculated sludge reactor.

**Table 1** | Operating conditions of the reactor cycle

Reactor	Inflow (min)	Aeration (min)	Settling (min)	Drainage (min)	Idle (min)	HRT (h)
S1,S2,S3	60	180	10 (5)	8	222 (227)	8
R2	60	180	60	8	172	8

## 2.2. Inoculated sludge and influent

The sludge used for inoculation was obtained from the second sewage treatment plant in Shangjie District (Zhengzhou, China). The inoculated activated sludge was in a brownish-yellow flocculent state with the MLSS of 8,130 mg·L<sup>-1</sup>. Before inoculation, larger impurities were removed using a sieve. The composition of synthetic wastewater is shown in Table 2. CH<sub>3</sub>COONa and KH<sub>2</sub>PO<sub>4</sub> were used as the carbon source and the phosphate source, respectively. The synthetic wastewater used in this study included (per liter): 0.434 g CH<sub>3</sub>COONa (COD = 330 mg·L<sup>-1</sup>), 0.172 g NH<sub>4</sub>Cl (NH<sub>4</sub><sup>+</sup>-N = 43 mg·L<sup>-1</sup>), 0.029 g KH<sub>2</sub>PO<sub>4</sub> (PO<sub>4</sub><sup>3-</sup>-P = 6.9 mg·L<sup>-1</sup>), 0.040 g MgSO<sub>4</sub>, 0.080 g CaCl<sub>2</sub>·2H<sub>2</sub>O and 1.0 mL trace elements solution, 1 L nutrient solution consisted of 1.5 g of FeCl<sub>3</sub>·6H<sub>2</sub>O, 0.15 g of H<sub>3</sub>BO<sub>3</sub>, 0.03 g of CuSO<sub>4</sub>·5H<sub>2</sub>O, 0.18 g of KI, 0.12 g of MnCl<sub>2</sub>·4H<sub>2</sub>O, 0.06 g of Na<sub>2</sub>MoO<sub>4</sub>·2H<sub>2</sub>O, 0.12 g of ZnSO<sub>4</sub>·7H<sub>2</sub>O, 0.15 g of CoCl<sub>2</sub>·6H<sub>2</sub>O, and 10 g of EDTA. All the above chemicals were purchased from Sinopharm Group Co. Ltd (China).

## 2.3. Test measurement

All the water samples were filtered through a 0.45 μm filter paper and analyzed immediately. COD, NH<sub>4</sub><sup>+</sup>-N, NO<sub>2</sub><sup>-</sup>-N, NO<sub>3</sub><sup>-</sup>-N, and PO<sub>4</sub><sup>3-</sup>-P were measured by standard methods (Rice 2012). Mixed liquor suspended solids (MLSS), mixed liquor volatile suspended solids (MLVSS), and sludge volumetric index (SVI) were analyzed according to APHA standard methods (Apha 1998). DO and pH were measured by WTW Multi 3401 DO tester. The determination of sludge particle size was carried out using a laser particle size analyzer (Bettersize BT9300H).

## 2.4. Extraction and analysis of extracellular polymeric substances

Extracellular polymeric substances (EPSs) were extracted as follows: (1) 30 mL of mixture was taken after aeration, and centrifuged with 6,000 rpm at 4 °C for 10 min; (2) the concentrated mixture was washed with distilled water for 2–3 times, followed by the addition of 0.5% NaCl solution and homogenized; (3) the sample was heated in a 60 °C water bath for 45 min, and centrifuged with 20,000 rpm at 20 °C for 10 min. Finally, the supernatant was separated as EPS solution (Seviour *et al.* 2009). Polysaccharide (PS) was measured using the phenol sulfuric method with glucose as the standard (Liu & Fang 2002). Protein (PN) content was measured following the modified Lowry Folin method with bovine serum albumin (BSA) as the standard (Frolund *et al.* 1995).

## 2.5. High-throughput sequencing

At the 80th day, sludge samples were collected from the S1, S2, S3, and R2 reactors for microbial community analysis. The characteristics and differences in microbial community structure were determined by 16S rDNA gene sequencing technology. The high-throughput sequencing was conducted by Bio-engineering (Shanghai) Co., Ltd (Shanghai, China).

## 3. RESULTS AND DISCUSSION

### 3.1. Comparison of sludge granulation effect

The average particle sizes and percentage of granular sludge were measured during the experimental period. Simultaneously, the MLSS and SVI of the sludge were monitored to assess its settling characteristics (Figure 2). The average particle size of the sludge inoculated was 82.84 μm, with sludge particles larger than 200 μm accounting for 3.74%. As the experiments

**Table 2** | Synthetic wastewater quality

S1, S2, S3, and R2	COD (mg·L <sup>-1</sup> )	NH <sub>4</sub> <sup>+</sup> -N (mg·L <sup>-1</sup> )	PO <sub>4</sub> <sup>3-</sup> -P (mg·L <sup>-1</sup> )	C/N	Time (d)
Concentration	330	43	6.9	7.6	1–80

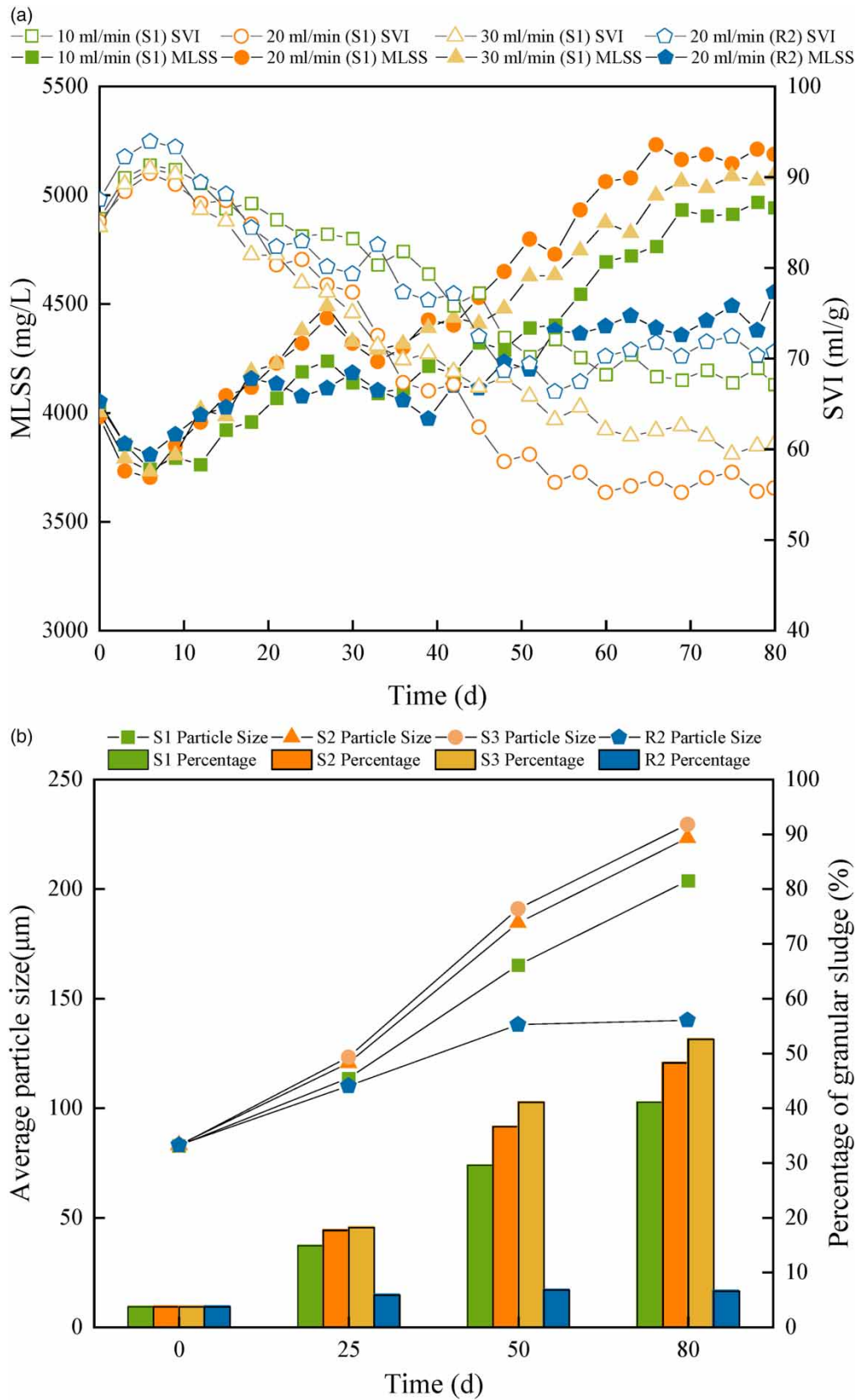


Figure 2 | MLSS, SVI (a) and granular sludge content (b) for S1, S2, and S3.

progressed, there was a significant increase in the particle sludge content and average particle size in reactors S1, S2, and S3, while reactor R2 showed only a slight increase. Furthermore, the particle sludge content and average particle size were found to be directly proportional to the micro-bubble aeration intensity. By the 80th day of the experiment, the particle sludge percentage in S1, S2, S3, and R2 were 41.10, 48.30, 52.60, and 6.6%, respectively, with the average diameter of 203.7, 223.3, 229.6, and 104.0  $\mu\text{m}$ , respectively. S1, S2, and S3 exhibited a state of floc–granule sludge coexistence. The initial MLSS in the reactors was around  $4,000 \text{ mg}\cdot\text{L}^{-1}$ . The MLSS decreased only during the initial phase of the experiment (also from the 25th to 38th day when sedimentation time was reduced), and it steadily increased during the rest period. The average MLSS of S1, S2, S3, and R2 throughout the entire experimental period were 4,324, 4,535, 4,475, and  $4,187 \text{ mg}\cdot\text{L}^{-1}$ , respectively. Different aeration intensities resulted in different granulation effects, and further affected the MLSS. The SVI only showed a slight increase in the early stages and gradually decreased as the granular sludge formed. The reduction in sedimentation time showed no significant effect on the sludge settling performance. On the 80th day, the SVI of S1, S2, S3, and R2 were 67.12, 55.67, 60.43, and  $70.67 \text{ mL}\cdot\text{g}^{-1}$ , respectively. The presence of granular sludge resulted in significantly better settling characteristics. Controlling the sedimentation time can effectively promote the formation of granules in SBAR, and the aeration intensity was positively correlated with the granulation process. However, when aeration intensity increased from 20 to  $30 \text{ mL}\cdot\text{min}^{-1}$  further, its effect on granulation was limited.

### 3.2. EPS content and composition

The secretion of EPS by microorganisms plays a crucial role in initiating the aerobic granulation process by aggregating bacterial cells and other particulate matter, contributing to the structural integrity of AGS (Lin *et al.* 2010). The composition of EPS is equally important in sludge flocculation, and the improvement of flocculation performance is associated with the extracellular protein PN (Flemming & Wingender 2001). The EPS content and PN/PS ratio of each reactor are shown in Figure 3.

Under different aeration intensities, the EPS content of S1, S2, and S3 gradually increased from 37.52, 35.72, and  $37.19 \text{ mg}\cdot(\text{g}\cdot\text{MLSS})^{-1}$  to 136.77, 149.85, and  $164.90 \text{ mg}\cdot(\text{g}\cdot\text{MLSS})^{-1}$ , respectively. This is consistent with the significant increase

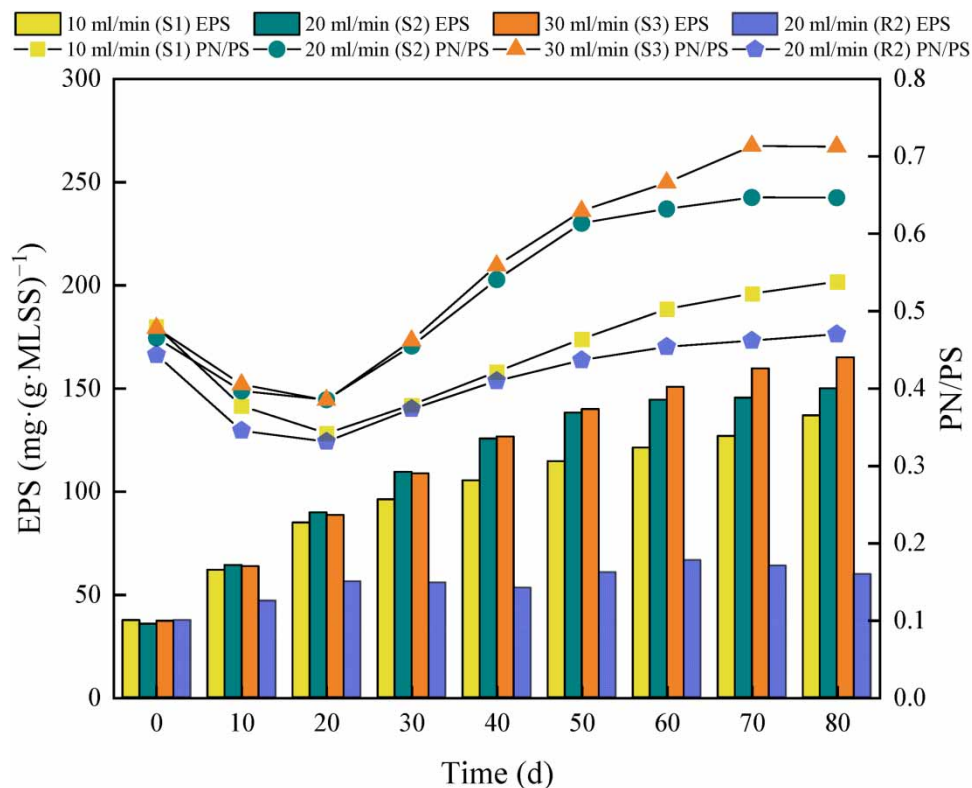


Figure 3 | EPS content and PN/PS in S1, S2, and S3 reactors.

in EPS content observed in many studies during the granulation process (Adav *et al.* 2008; Xu *et al.* 2020). Aeration intensity influenced the hydraulic shear force. When the aeration intensity increased, microorganisms secreted a large amount of EPS to mitigate the destructive effects of high shear forces on their structure and activity (Bruckner *et al.* 2011; Remmas *et al.* 2017). This may have been the reason for the highest EPS content observed in the S3 system. Compared to the other three reactors, R2 exhibited a slower increase in EPS, which could be attributed to its lower content of granular sludge. PN, as a hydrophobic substance on the surface of AGS, enhanced the aggregation of microorganisms, while PS, as a hydrophilic substance, promoted the adhesion between microorganisms. Therefore, the sedimentation and stability of AGS increased with the concentration of PN or the PN/PS ratio (Zhu *et al.* 2012). In the initial stage of sludge granulation (before the 20th day), the growth rate of PS was relatively faster, and the PN/PS ratio in S1, S2, S3 and R2 decreased from 0.48, 0.47, 0.48 and 0.44 to 0.34, 0.38, 0.38, and 0.34, respectively. Subsequently, as the sludge particles entered the rapid growth phase, the growth rate of PN exceeded that of PS, resulting in a rapid increase in the PN/PS ratio. In the later stages, as the granular sludge content kept constant, the increase in the PN/PS ratio also slowed down. By the end of the experiment, the PN/PS ratios in S1, S2, and S3 were 0.54, 0.65, and 0.71, respectively. Meanwhile, the PN/PS ratio in the R2 reactor was the lowest at 0.47. These viscous EPS promoted the aggregation of microorganisms and were one of the key factors in the formation of AGS. Under the same influent conditions, the PN content was positively correlated with the aeration intensity. Therefore, a higher aeration intensity facilitated the secretion of EPS and increased the PN content, playing an important role in the formation of AGS. However, high aeration intensity inevitably lead to higher energy consumption, and further evaluation of the pollutant removal of each reactor is needed to determine the appropriate aeration intensity.

### 3.3. Comparison of pollutant removal performance

The experiment evaluated the removal efficiency of nutrients in the S1, S2, and S3, and compared them with the R2 (Figure 4). At aeration intensities of 10, 20, and 30 mL·min<sup>-1</sup>, the average DO in the aeration phase was approximately 5, 6, and 7 mg·L<sup>-1</sup>, respectively, with differences of around 1 mg·L<sup>-1</sup>. At the early stage of the experiment, the predominant form of sludge was flocs, and the NH<sub>4</sub><sup>+</sup>-N removal efficiencies of the S1, S2, S3, and R2 systems were 85.47, 86.06, 86.26, and 85.93%, respectively. After 20 days of operation, the NH<sub>4</sub><sup>+</sup>-N removal efficiencies of all systems exceeded 90%, and a small amount of granular sludge had formed in the S1, S2, and S3 systems. By the end of the operation period (80 days), the effluent NH<sub>4</sub><sup>+</sup>-N concentration approached nearly 0 mg·L<sup>-1</sup>, indicating that all reactors had good NH<sub>4</sub><sup>+</sup>-N removal capabilities, and the differences in removal efficiency were limited.

The inherent oxygen gradient in granular sludge facilitated simultaneous nitrification–denitrification. Some NH<sub>4</sub><sup>+</sup>-N was oxidized to NO<sub>3</sub><sup>-</sup>-N at the surface of the granules and immediately reduced to N<sub>2</sub> within the granule, the formation of granular sludge promotes the removal of TN from the system. On the 5th day, the TN removal efficiencies of the S1, S2, S3, and R2 were 48.35, 48.52, 49.02, and 50.05%, respectively, and then all gradually increased. By the 80th day, the TN removal efficiencies of S1, S2, S3, and R2 were 70.21, 77.23, 74.33, and 67.54%, respectively. The TN removal efficiency of the floc–granule sludge coexisted system was higher than that of the floc sludge system. However, excessive aeration intensity may increase the depth of dissolved oxygen transfer, inhibiting the denitrification process (Beun *et al.* 2001) which could explain why S2 exhibited the highest TN removal efficiency.

In addition to being consumed by denitrifying bacteria, organic matter was also absorbed by polyphosphate-accumulating organism (PAO) during the influent anaerobic stage, where it was used for synthesizing poly-β-hydroxyalkanoates (PHAs) to release phosphorus. Due to the structure of granular sludge which was more favorable for the growth of phosphorus removing bacteria, the COD removal efficiencies of S1, S2, and S3 were slightly higher than that of R2. At the end of the cultivation period, the COD removal efficiencies of the S1, S2, S3, and R2 were 95.1, 96.3, 95.6, and 89.7%, respectively. Initially, the TP removal efficiency was around 60%, and it gradually increased as the PAO enriched. The unique hierarchical structure of granular sludge was more conducive to collaboration between PAO. By the 25th day, the TP removal efficiencies of the S1, S2, S3, and R2 were 62.64, 67.78, 65.03, and 63.87%, respectively. On the 25th day, due to a sharp decreased sludge settling time, some sludge was run off, resulting in a temporary deterioration of phosphorus removal performance. With the formation of granular sludge, the TP removal efficiency of S1, S2, and S3 all became better compared to R2. By the 80th day, the TP removal efficiencies of S1, S2, S3, and R2 were 81.22, 89.50, 85.91, and 75.89%, respectively. S2 had the highest TP removal efficiency, while the phosphorus removal in S3 might be affected by excessive aeration. Excessive aeration led to insufficient PHAs within the PAO, and excessive carbon sources would be utilized for denitrification. When the PAO

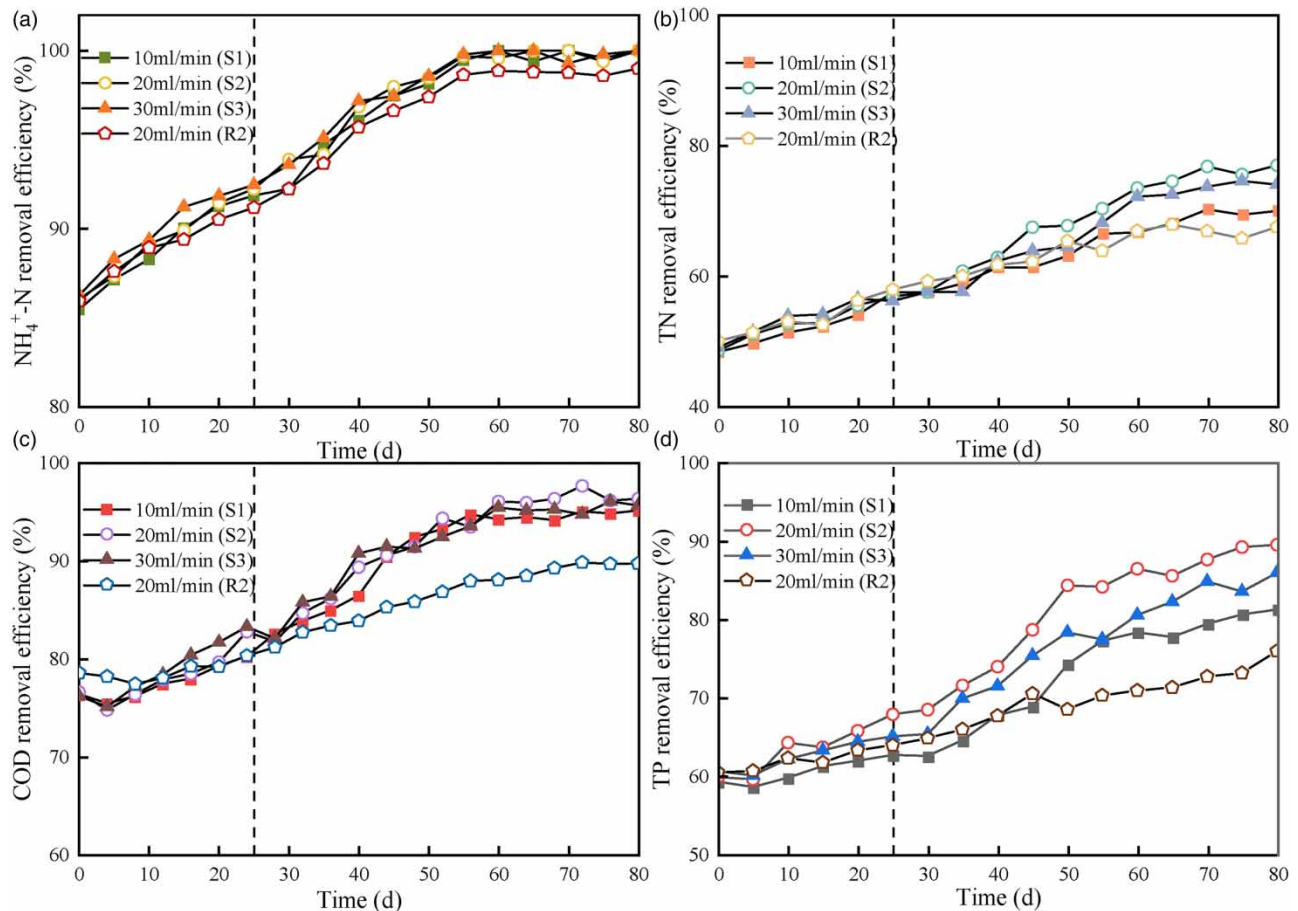


**Figure 4** |  $\text{NH}_4^+\text{-N}$  (a), TN (b), COD (c), and TP (d) removal efficiency in S1, S2, S3, and R2.

were in a famine condition, the phosphorus uptake reaction will be finished, resulting in a decrease in the phosphorus removal performance. The micro-bubble aeration floc–granule sludge coexistence system showed a better removal efficiency of nutrients than the traditional coarse-bubble aeration floc-based sludge system. COD was already at a low level before the idle stage, and only limited denitrification occurred during the idle stage, with little change in phosphorus concentration.

### 3.4. Microbial community structure analysis

Shannon's index is positively correlated with community diversity, while Simpson's index is inversely correlated with community diversity. The Shannon's indices of the S1, S2, S3, and R2 were 5.17, 5.03, 4.88, and 5.12, respectively, while the Simpson's indices were 0.019, 0.025, 0.029, and 0.016, respectively. In the granulation process, various non-adaptive microorganisms were eliminated (Lv *et al.* 2014), leading to a simpler community structure in reactors S1, S2, and S3 compared to R2. The differences in community structure at different aeration intensities were likely attributed to variations in their granular sludge content. The microbial community structure at the end of operation of each reactor is shown in Figure 5.

In AGS, various microorganisms, such as nitrifying bacteria, denitrifying bacteria, PAO, and denitrifying PAO, synergistically remove organic carbon, nitrogen, and phosphorus (Yan *et al.* 2019). *Nitrosomonas*, as a representative ammonia-oxidizing bacteria (AOB), oxidizes  $\text{NH}_4^+\text{-N}$  to  $\text{NO}_3^-\text{-N}$  (Li *et al.* 2017). The relative abundance of *Nitrosomonas* in the S1, S2, S3, and R2 were 0.09, 0.11, 0.14, and 0.05%, respectively, and its abundance increased with the increase of aeration intensity. Additionally, under the same aeration intensity, the abundance of *Nitrosomonas* was slightly higher in the granular sludge compared to the floc sludge. *Nitrospira*, a common genus of nitrite-oxidizing bacteria (NOB), had the highest abundance in S2 (2.32%), higher than S1 (1.06%) and S3 (0.99%), and the lowest abundance in R2 (0.14%). Denitrifying bacteria, such as *Azoarcus* (2.95–12.17%), *Ferruginibacter* (2.08–6.19%), *Hydrogenophaga* (1.82–3.94%), and *Thauera*



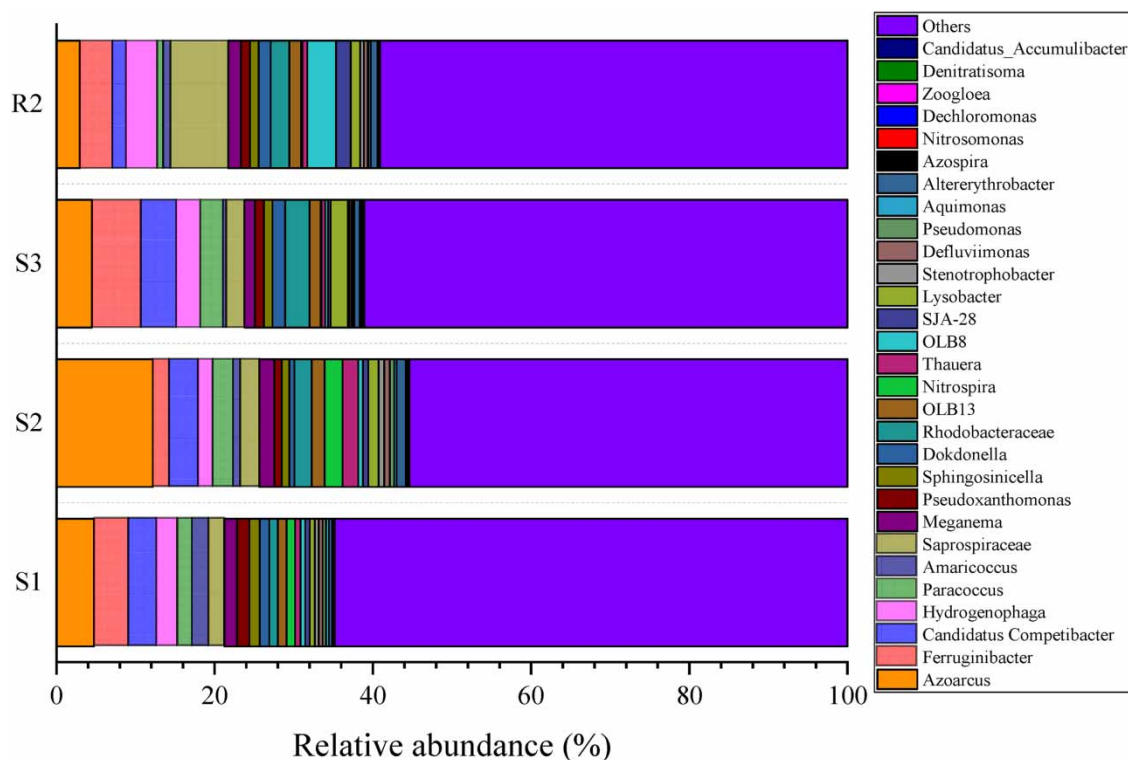


**Figure 5** | Microbial community structure at the genus level S1, S2, S3, and R2.

(0.43–1.95%) were distributed in all four systems, and their abundance did not show a clear relationship with aeration intensity. Among them, *Azoarcus* has the highest abundance in S2 (12.17%). PAOs store volatile fatty acids under anaerobic conditions for synthesizing PHAs and accumulate phosphorus under aerobic conditions (Filipe *et al.* 2001). PAOs, such as *Paracoccus*, were distributed in all four systems, with the highest abundance in S3 at 2.89%, higher than S1 (1.85%), S2 (2.60%), and R2 (0.76%). Glycogen-accumulating organisms (GAOs), such as *Candidatus competibacter* (1.72–4.49%), also had the highest abundance in S3, utilizing VFAs for PHA synthesis but without phosphorus accumulation (Filipe *et al.* 2001). They compete with PAOs, which might explain the higher abundance of *Paracoccus* in S3 but lower TP removal efficiency compared to S2. *Pseudomonas*, a type of denitrifying PAOs, can simultaneously denitrify and take up phosphorus, achieving synchronous removal of nitrogen and phosphorus (He & McMahon 2011; He *et al.* 2016). It is more abundant in the internal anoxic environment of granular sludge (Alves *et al.* 2022). Its abundance in the granular sludge system was significantly higher, which explained the relatively higher TP removal efficiencies in S1, S2, and S3. The floc–granule sludge system is more conducive to the enrichment of nitrifying bacteria, denitrifying bacteria, and PAO, resulting in the bigger relative abundances.

### 3.5. Mechanism and energy-saving analysis

The transformation of floc sludge into a floc–granule coexistence sludge was more conducive to the removal of pollutants, and the nutrients removal mechanism is shown in Figure 6. The variations of  $\text{NH}_4^+\text{-N}$  in typical cycles of S2 and R2 at the end of the experiment were recorded respectively, and the aeration time required to reduce the  $\text{NH}_4^+\text{-N}$  to  $5 \text{ mg}\cdot\text{L}^{-1}$  (Class I A emission standard, GB18918-2016) was calculated, as shown in Figure 7. Due to the low COD concentration in the aeration stage, only the nitrification process was considered for energy saving. The theoretical energy-saving aeration consumption was evaluated by comparing the aeration time between S2 and R2, as shown in Table 3.

For the conventional aeration floc sludge system, the aeration time needed to nitrify  $\text{NH}_4^+\text{-N}$  to  $5 \text{ mg}\cdot\text{L}^{-1}$  was approximately 1.25 h. In contrast, for the floc–granule coexistence system operated with micro-bubble aeration, the required aeration time was approximately 1.07 h, which was about 85.6% of the conventional system. Consequently, the theoretical energy-saving potential was estimated to be 14.4%. Furthermore, based on the calculated aeration time, the nitrification rates were

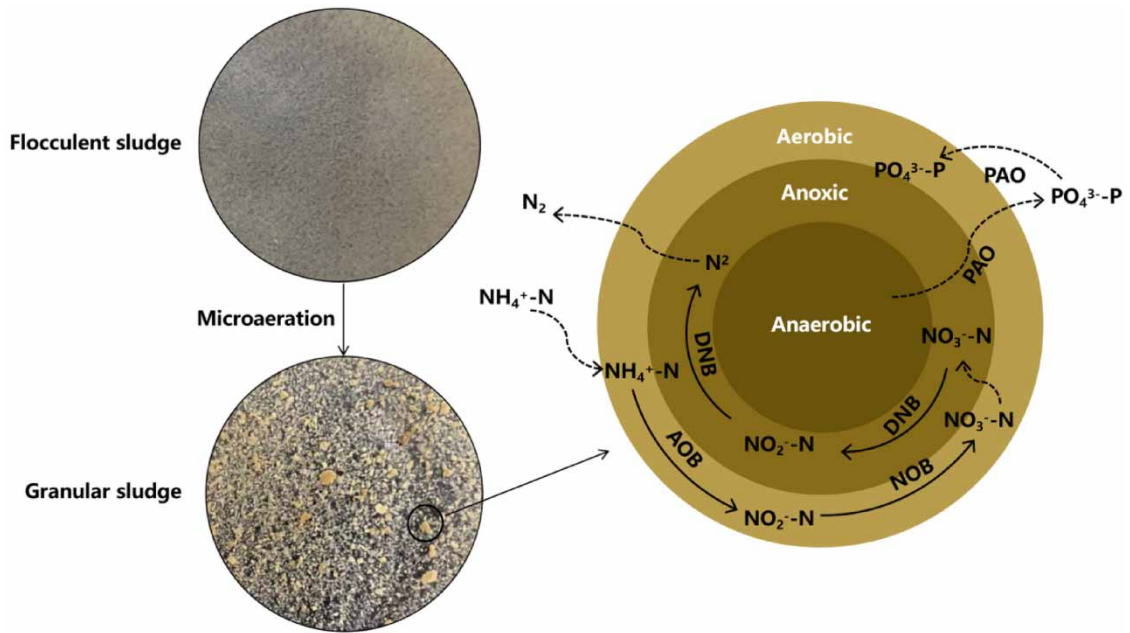


**Figure 6** | Sludge morphology changes and pollutant removal mechanisms.

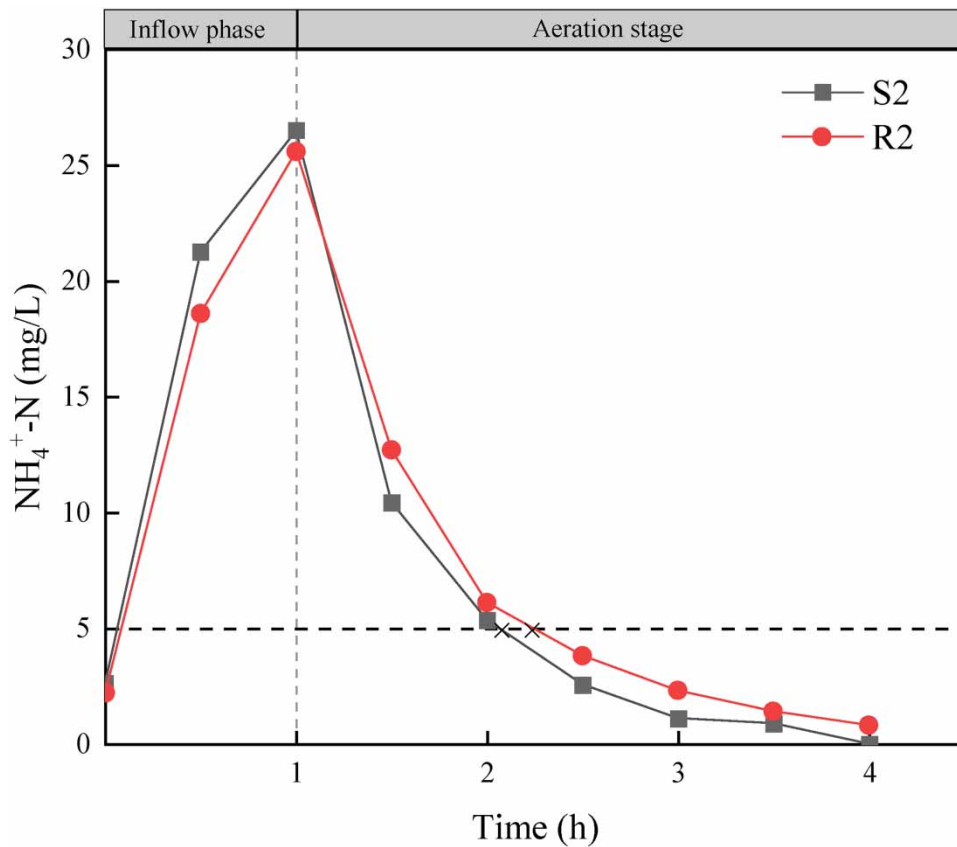


**Figure 7** | Variation of  $\text{NH}_4^+-\text{N}$  concentration in typical cycle of S2 and R2 reactors.

**Table 3** | Comparison of theoretical energy consumption of S2 and R2

Reactor	Effective aeration time (h)	MLSS (mg/L)	Specific nitrification rate (mg·(gVSS·h) <sup>-1</sup> )	Energy consumption comparison (%)	Theoretical energy consumption reduction (%)
R2	1.25	5,188	3.14	100	0
S2	1.07	4,577	3.54	85.6	14.4

determined to be 3.14 mg·(gVSS·h)<sup>-1</sup> for R2 and 3.54 mg·(gVSS·h)<sup>-1</sup> for S2. Combining the analysis above, the micro-bubble floc–granule coexistence system demonstrated better treatment performance with a higher abundance of nutrients removal bacteria, presenting significant advantages over the conventional coarse-bubble aeration floc sludge system. However, the cost of microporous aeration equipment is higher than that of ordinary aeration equipment. Therefore, the development of low-cost anti-clogging microporous aeration equipment is the future development direction of this process.

#### 4. CONCLUSION

A coexistence system of floc-granular sludge was successfully developed in micro-bubble aeration SBAR. The best granulation performance was achieved under the aeration intensity of 30 mL·min<sup>-1</sup>, with a granular sludge content of 52.60%. However, better nutrients removal performance was observed at 20 mL·min<sup>-1</sup>, with NH<sub>4</sub><sup>+</sup>-N, TN, and TP removal efficiencies of 100, 77.0, and 89.5%, respectively. Compared to the coarse-bubble floc sludge system, the floc–granule coexistence system exhibited simpler microbial community structure but higher abundance of nutrients removal bacteria. By combining micro-bubble aeration with AGS, it is possible to improve the effluent quality as well as saving energy consumption.

#### FUNDING

This research was funded by the National Natural Science Foundation of China (No. 42107427 and No. 42377375) and the Science and Technology Foundation of Henan Province (No. 222102320426).

#### DATA AVAILABILITY STATEMENT

All relevant data are included in the paper or its Supplementary Information.

#### CONFLICT OF INTEREST

The authors declare there is no conflict.

#### REFERENCES

- Adav, S. S., Lee, D. J. & Tay, J. H. 2008 Extracellular polymeric substances and structural stability of aerobic granule. *Water Research*. <https://doi.org/10.1016/j.watres.2007.10.013>.
- Alves, O. I. M., Araujo, J. M., Silva, P. M. J., Magnus, B. S., Gavazza, S., Florencio, L. & Kato, M. T. 2022 Formation and stability of aerobic granular sludge in a sequential batch reactor for the simultaneous removal of organic matter and nutrients from low-strength domestic wastewater. *Science of the Total Environment*. <https://doi.org/10.1016/j.scitotenv.2022.156988>.
- Apha. 1998 *Standard Methods for the Examination of Water and Wastewater*. American Public Health Association, Washington, DC, USA.
- Bassin, J. P., Kleerebezem, R., Dezotti, M. & van Loosdrecht, M. C. 2012 Measuring biomass specific ammonium, nitrite and phosphate uptake rates in aerobic granular sludge. *Chemosphere*. <https://doi.org/10.1016/j.chemosphere.2012.07.050>.
- Beun, J. J., Heijnen, J. J. & van Loosdrecht, M. C. 2001 N-removal in a granular sludge sequencing batch airlift reactor. *Biotechnology and Bioengineering*. <https://doi.org/10.1002/bit.1167>.
- Bruckner, C. G., Rehm, C., Grossart, H.-P. & Kroth, P. G. 2011 Growth and release of extracellular organic compounds by benthic diatoms depend on interactions with bacteria. *Environmental Microbiology*. <https://doi.org/10.1111/j.1462-2920.2010.02411.x>.
- Chen, C., Bin, L., Tang, B., Huang, S., Fu, F., Chen, Q., Wu, L. & Wu, C. 2017 Cultivating granular sludge directly in a continuous-flow membrane bioreactor with internal circulation. *Chemical Engineering Journal*. <https://doi.org/10.1016/j.cej.2016.10.034>.
- Cheng, X., Xie, Y., Zheng, H., Yang, Q., Zhu, D. & Xie, J. 2016 Effect of the different shapes of air diffuser on oxygen mass transfer coefficients in microporous aeration systems. *Procedia Engineering*. <https://doi.org/10.1016/j.proeng.2016.07.599>.
- Filipe, C. D., Daigger, G. T. & Grady Jr, C. P.. 2001 Stoichiometry and kinetics of acetate uptake under anaerobic conditions by an enriched culture of phosphorus-accumulating organisms at different pHs. *Biotechnology and Bioengineering*. <https://doi.org/10.1002/bit.1023>.

- Flemming, H. C. & Wingender, J. 2001 Relevance of microbial extracellular polymeric substances (EPSs) - part II: Technical aspects. *Water Science and Technology*. <https://doi.org/10.2166/wst.2001.0328>.
- Frolund, B., Griebe, T. & Nielsen, P. H. 1995 Enzymatic activity in the activated-sludge floc matrix. *Applied Microbiology and Biotechnology*. <https://doi.org/10.1007/BF00164784>.
- He, S. & McMahon, K. D. 2011 Microbiology of 'Candidatus Accumulibacter' in activated sludge. *Microbial Biotechnology*. <https://doi.org/10.1111/j.1751-7915.2011.00248.x>.
- He, Q., Zhou, J., Wang, H., Zhang, J. & Wei, L. 2016 Microbial population dynamics during sludge granulation in an A/O/A sequencing batch reactor. *Bioresource Technology*. <https://doi.org/10.1016/j.biortech.2016.04.088>.
- Kartal, B., Kuenen, J. G. & van Loosdrecht, M. C. 2010 Engineering. Sewage treatment with anammox. *Science*. <https://doi.org/10.1126/science.1185941>.
- Khuntia, S., Majumder, S. K. & Ghosh, P. 2012 Microbubble-aided water and wastewater purification: A review. *Reviews in Chemical Engineering*. <https://doi.org/10.1515/revce-2012-0007>.
- Li, Y., Liu, Y., Shen, L. & Chen, F. 2008 DO diffusion profile in aerobic granule and its microbiological implications. *Enzyme and Microbial Technology*. <https://doi.org/10.1016/j.enzmictec.2008.04.005>.
- Li, J., Zhang, L., Peng, Y. & Zhang, Q. 2017 Effect of low COD/N ratios on stability of single-stage partial nitrification/anammox (SPN/A) process in a long-term operation. *Bioresource Technology*. <https://doi.org/10.1016/j.biortech.2017.07.127>.
- Lin, Y., de Kreuk, M., van Loosdrecht, M. C. & Adin, A. 2010 Characterization of alginate-like exopolysaccharides isolated from aerobic granular sludge in pilot-plant. *Water Research*. <https://doi.org/10.1016/j.watres.2010.03.019>.
- Liu, H. & Fang, H. H. 2002 Extraction of extracellular polymeric substances (EPS) of sludges. *Journal of Biotechnology*. [https://doi.org/10.1016/s0168-1656\(02\)00025-1](https://doi.org/10.1016/s0168-1656(02)00025-1).
- Liu, X. W., Sheng, G. P. & Yu, H. Q. 2009 Physicochemical characteristics of microbial granules. *Biotechnology Advances*. <https://doi.org/10.1016/j.biotechadv.2009.05.020>.
- Lv, Y., Wan, C., Lee, D. J., Liu, X. & Tay, J. H. 2014 Microbial communities of aerobic granules: Granulation mechanisms. *Bioresource Technology*. <https://doi.org/10.1016/j.biortech.2014.07.005>.
- Remmas, N., Melidis, P., Zerva, I., Kristoffersen, J. B., Nikolaki, S., Tsiamis, G. & Ntougias, S. 2017 Dominance of candidate Saccharibacteria in a membrane bioreactor treating medium age landfill leachate: Effects of organic load on microbial communities, hydrolytic potential and extracellular polymeric substances. *Bioresource Technology*. <https://doi.org/10.1016/j.biortech.2017.04.019>.
- Rice 2012 *Standard Methods for the Examination of Water and Wastewater*. American Public Health Association, Washington, DC, USA.
- Seviour, T., Pijuan, M., Nicholson, T., Keller, J. & Yuan, Z. 2009 Gel-forming exopolysaccharides explain basic differences between structures of aerobic sludge granules and floccular sludges. *Water Research*. <https://doi.org/10.1016/j.watres.2009.07.018>.
- Show, K.-Y., Lee, D.-J. & Tay, J.-H. 2012 Aerobic granulation: Advances and challenges. *Applied Biochemistry and Biotechnology*. <https://doi.org/10.1007/s12010-012-9609-8>.
- Wang, W., Wang, X., Wang, S. & Li, J. 2018 Partial denitrification coupled with immobilization of anammox in a continuous upflow reactor. *RSC Advances*. <https://doi.org/10.1039/c8ra05649h>.
- Xu, D., Li, J., Liu, J. & Ma, T. 2020 Rapid aerobic sludge granulation in an integrated oxidation ditch with two-zone clarifiers. *Water Research*. <https://doi.org/10.1016/j.watres.2020.115704>.
- Yan, L., Liu, S., Liu, Q., Zhang, M., Liu, Y., Wen, Y., Chen, Z., Zhang, Y. & Yang, Q. 2019 Improved performance of simultaneous nitrification and denitrification via nitrite in an oxygen-limited SBR by alternating the DO. *Bioresource Technology*. <https://doi.org/10.1016/j.biortech.2018.12.054>.
- Zhou, D., Niu, S., Xiong, Y., Yang, Y. & Dong, S. 2014 Microbial selection pressure is not a prerequisite for granulation: Dynamic granulation and microbial community study in a complete mixing bioreactor. *Bioresource Technology*. <https://doi.org/10.1016/j.biortech.2014.03.001>.
- Zhu, L., Lv, M. L., Dai, X., Yu, Y. W., Qi, H. Y. & Xu, X. Y. 2012 Role and significance of extracellular polymeric substances on the property of aerobic granule. *Bioresource Technology*. <https://doi.org/10.1016/j.biortech.2011.12.008>.

First received 8 September 2023; accepted in revised form 9 November 2023. Available online 21 November 2023